PHYSICAL REVIEW B

SOLID STATE

THIRD SERIES, VOL. 4, NO. 12 15 DECEMBER 1971

Specific Heat of Gold-Zinc Alloys below 3 °K

Douglas L. Martin

Division of Physics, National Research Council of Canada, Ottawa, Canada

(Received 15 July 1971)

The electronic specific heat is found to initially increase on adding zinc to gold, in agreement with recent work of Clune and Green who relate this behavior to changes in the electron-phonon enhancement factor superimposed on a rigid-band model. The results for a 7.5-at.%-Zn alloy were stable against drastic changes in heat treatment, whereas those for a 10-at.% alloy were very dependent on heat treatment. It is therefore postulated that the α-phase region extends only to ~ 9 at.% at room temperature, contrary to recent phase diagrams. The results at 10 at.% Zn also suggest that very slow cooling retains a large part of the α phase, but quenching produces the ordered phase. A possible explanation is that the high lattice-vacancy concentration immediately after quenching facilitates atomic movement.

INTRODUCTION

The electronic specific heat of alloys has been of considerable experimental and theoretical interest. Green and collaborators have done a great deal of experimental work on noble-metal alloys and Will and Green[1] concluded that the electronic specific-heat coefficient γ always initially increased when a polyvalent nontransition metal was alloyed with a noble metal. Clune and Green[2] have more recently explained this result as the effect of changes in the electron-phonon enhancement factor superimposed on a rigid-band model. The present author had published[3] data on an Au–10-at.%-Zn alloy and it was noted that the significant decrease of γ which was observed was contrary to the above-mentioned[1] empirical rule. The explanation[2] of this rule prompted further work on the Au-Zn system.

EXPERIMENTAL

The 10-at.%-Zn alloy was that which was used in the previous work.[3] The other alloys were prepared, cleaned, degassed, homogenized, and analyzed as described previously.[3] Sample details will be found in Table I. Measurements were made in the same apparatus as used before.[3] The error limits tabulated in the present paper are 95% confidence limits from the statistical analysis. The absolute accuracy[3] is estimated to be 0.4% plus the statistical error plus error arising from uncertainty in the composition (and therefore average atomic weight). The atomic weight from the composition analysis was used in evaluating the data for the 5.0-at.%-Zn sample, and from the first composition analysis for all the 10.0-at.%-Zn sample results. For the 2.5-at.%-Zn sample the composition analysis agreed exactly with the nominal composition. The nominal atomic weight was used in evaluating results for the 7.5-at.%-Zn sample. The data used was determined by the availability of the composition analysis at the time of computation. Reference to Table I shows that errors should not exceed $\pm 0.1\%$.

RESULTS

The specific-heat (C_p) data were fitted to the equation

$$C_p = HT^{-2} + \gamma T + [464.34/(\Theta_0^c)^3]\, T^3 + BT^5,$$

where H is the coefficient of the nuclear specific-heat term and Θ_0^c is the low-temperature limiting value of the Debye temperature. The values of the coefficients are given in Table II and deviations of the experimental results from the combined fit of both runs are shown in Fig. 1. For the 10-at.%-Zn sample the data for runs 1 and 2 are not shown, having been illustrated previously.[3]

For the 2.5-at.%-Zn sample there was an interval of six weeks between the heat treatment and the first run and then five weeks before the second run. For the 5.0-at.%-Zn sample the interval between heat treatment and first run was again about six weeks with another week interval before the second

TABLE I. Sample details

Sample (at. % Zn)	Heat treatment immediately before measurement	Weight (g)	Composition analysis (at. % Zn)		Atomic weight		Difference (%)	Impurities ppm by weight								
				Mean	From composition analysis	Nominal		Semiquantitative spectrographic analysis					Quantitative spectrographic analysis			
								Ag	Cu	Mg	Fe	Si	Fe	Mn	Si	Al
2.5	Slow cool in furnace from 520 °C	179.644	2.52		193.677	193.677	0.0	0.1–0.6	...		see quantitative analysis					
			2.46	2.50				0.1–0.6	3–30.0				0.28	< 0.015	0.15	...
			2.52					0.1–0.6	...	0.02–0.2	→	→	0.30	< 0.015	0.19	...
													0.27	< 0.015	0.27	...
5.0	Slow cool in furnace from 900 to ~ 500 °C, then air cool	186.000	5.12	5.10	190.246	190.387	0.07	0.06–0.6	0.02–0.15				0.3	< 0.015	0.5	< 0.5
			5.09					0.24–2.4	0.3 –3.0		→	→	0.6	< 0.015	0.2	< 0.5
									...							
									...							
7.5	Slow cool in furnace from 520 °C	184.777	7.23		187.321	187.097	0.12	0.2–2.0	0.1 –1.2	0.02–0.2	→	→	0.16	< 0.015	0.22	...
			7.45	7.33				0.1–1.2	...	0.02–0.2			0.13	< 0.015	0.29	...
			7.32					0.1–0.6	...				0.12	< 0.015	0.11	...
	Quench from 860 °C	184.254														
10.0	Quench from 825 °C	187.163	10.16	10.03	183.775	183.807	0.02	0.3–3.0	0.3 –3.0	0.01–0.06	0.2–1.5	0.03–0.3	see semiquantitative			
			9.89					1.0–6.0	0.2 –2.0	0.01–0.06	0.2–1.5	0.03–0.3	←	←	analysis	
	Slow cool in furnace from 800 to ~ 500 °C, then air cool	187.152														
	Slow cool in furnace from 540 °C	178.171	9.94	9.85	184.005	183.807	0.11	0.1–0.6	0.2 –2.0				0.39	0.02	0.07	...
			9.75					0.3–3.0	1.0–12.0	0.02–0.20	→	→	0.31	0.02	0.12	...

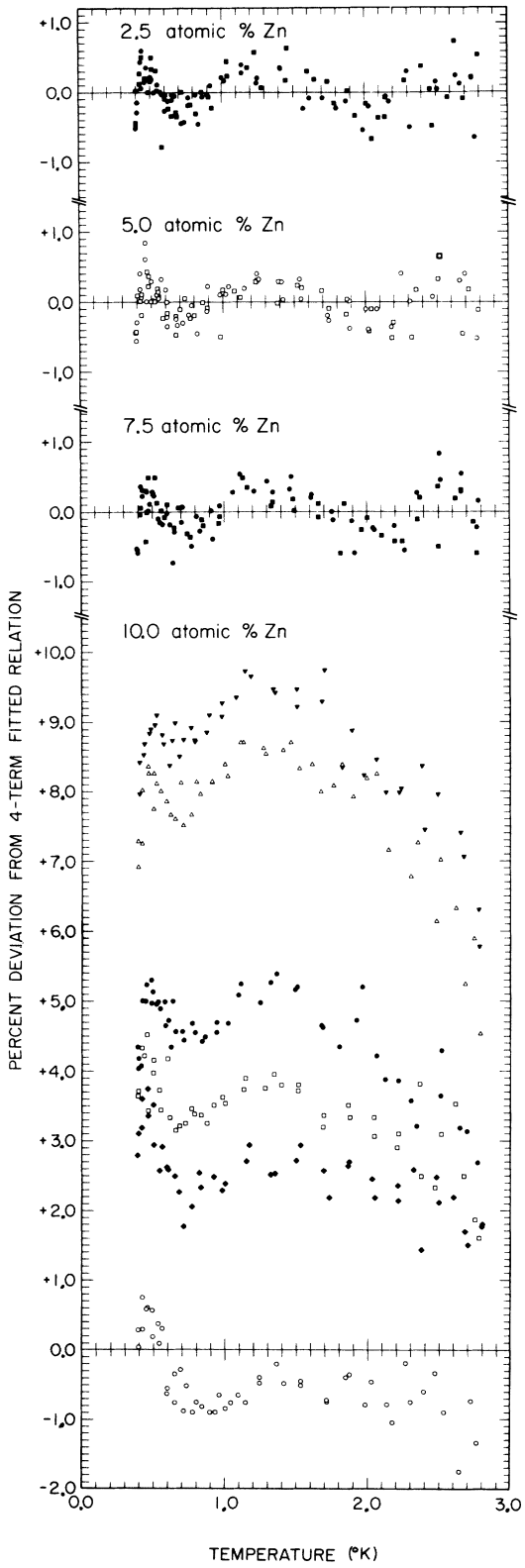

FIG. 1. Deviations of the individual results from the four-term fitted equations (see Table II and text).

run. The 7.5-at.%-Zn sample was run about five weeks after the slow cool and the day after the quench. The time from quenching to the start of cooling, preparatory to the run, was three hours. It will be noted that for each of these samples the results of of both runs are essentially identical.

For the 10.0-at.%-Zn sample the first two runs[3] were made four weeks after quenching and run 3 was made 28 months later (the sample having been stored at room temperature). The sample was then heated (in an alumina crucible in an evacuated quartz envelope) to about 800 °C for 17 h, cooled very slowly to about 500 °C, and then removed from the furnace and (still in the quartz envelope) allowed to cool to room temperature (air cool). Run 4 was made six days later, run 5 was made one week after run 4, and run 6 was made two weeks after run 5. It seemed possible, but unlikely, that the increase in the specific heat might be associated with some pickup of gas during heat treatment[4] and the sample was, therefore, degassed by heating in a vacuum under continuous pumping to 540 °C and then cooled very slowly by switching off the furnace. It will be seen that this treatment increased the specific heat still more (run 7 was made 10 days after the cool), but (run 8 was made 14 days later) the specific heat again decrea with time.

DISCUSSION

The results for the alloys containing 2.5, 5.0, and 7.5 at.% Zn will be considered first, noting that the last mentioned alloy is stable against drastic changes in heat treatment. It will therefore be assumed that these alloys are all in the α [face-centered-cubic (fcc)] phase.

Reference should be made to Fig. 2, where the results are plotted. The nuclear specific-heat coefficient is seen to increase smoothly with composition. The nuclear specific heat is believed to be associated with the nuclear electric quadruple moment and is therefore a measure of the electric field gradient at nuclear sites. The variation with composition is of the same form as was found in disordered Ag-Au alloys[5] and the absolute value correlates well with that found previously[3] for Au-Zn.

The electronic specific heat varies smoothly with composition. Within the given error limits the curve drawn through the data points could be replaced by a straight line with gradient 0.6 (μcal/°K^2 g atom)/at.% Zn. The present result, therefore, agrees qualitatively with the empirical rule of Will and Green[1] mentioned earlier. For the noble-metal alloys, Clune and Green[2] used a rough theoretical estimate of $d(\ln\lambda)/dZ$ (where λ is the electron-phonon enhancement factor and Z is the average number of valence electrons per atom) and a published theoretical estimate of $d\ln N(E_F)/dZ$

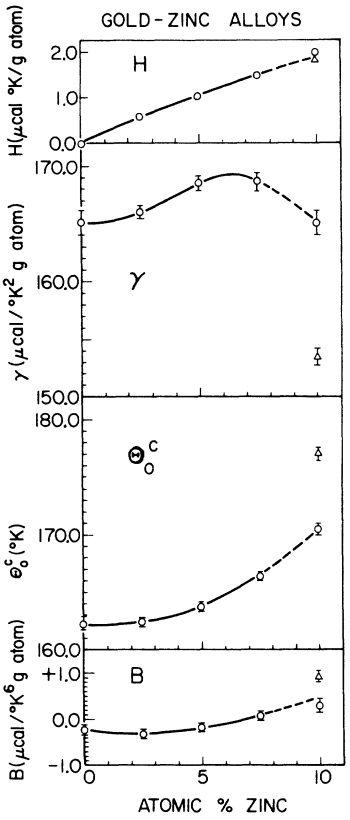

FIG. 2. Collected results from the analysis of specific-heat data (see Table II and text).

[where $N(E_F)$ is the density of states at the Fermi level] together with the experimentally observed $d(\ln\gamma)/dZ$ to obtain λ, which averages 0.33 for the noble-metal alloys they tabulate. The value obtained for Au-Zn from the present measurements, with the straight-line fit, mentional immediately above, is 0.30. Thus, the present results fit well with Clune and Green's theory.[2]

The lattice specific heat is represented by both Θ_0^c (T^3 term) and B (T^5 term) in Fig. 2. The smooth increase in Θ_0^c on alloying zinc with gold probably reflects the high-frequency "impurity" modes associated with the lighter zinc atoms, i.e., the low-frequency end of the lattice-vibration spectrum is depleted as zinc is added to gold. The unusual negative T^5 term found originally for pure gold[6] may initially become more negative on alloying but it then increases and becomes positive at about 7 at.% Zn.

The results obtained for the 10-at.%-Zn alloy will now be considered (refer to Fig. 1). The results of runs 1 and 2 on the quenched sample were published earlier[3] and differences from the least-squares fit to these runs are shown in Fig. 1. Run 3 shows that long storage at room temperature has resulted in a small decrease in specific heat. Fairly rapid cooling from ~500 °C has produced an increase in specific heat (run 4) and very slow cooling from ~500 °C produces an even greater increase (run 7). However, for both these situations, the alloy is then in an unstable condition and the specific heat decreases with time (runs 5, 6, and 8). The following explanation of these results is suggested. The published phase diagrams[7,8] for the Au-Zn system are incorrect and the α-phase region extends only to ~9 at.% at room temperature. The phase diagram shows that greater concentration of zinc would produce a mixture of the α (fcc) phase and the so-called $Au_{3+}Zn$ ordered phase. According to Iwasaki[9] this ordered phase can be derived from the fcc Cu_3Au-type ordered phase by introducing a two-dimensional antiphase domain structure with periods of 2 and 3 unit cells in the two directions which, in turn, results in atom shifts (lattice modulation). Since the 10-at.%-Zn alloy specific heat is observed to decrease with time, it appears that quenching from a high temperature has been most effective in producing the phase stable at room temperature, whereas very slow cooling has retained a great deal of the phase stable at higher temperatures (α phase). Some support for this argument can be obtained from Fig. 2, where it will be seen that results for the sample cooled very slowly are in best agreement with the extrapolated results from lower concentrations. The explanation for this behavior is probably that the low-temperature limit of the α phase at 10 at.% Zn is rather low (~100 °C) and transformation even just below this temperature is rather slow. However, the rapidly quenched alloy will contain an excess of (thermally generated) lattice vacancies which facilitate rapid atomic rearrangement.

To test this hypothesis further, some powder was filed from the 7.5 and 10-at.%-Zn samples. Each sample was cleaned with a magnet and placed in an alumina crucible which was then sealed in an evacuated quartz tube. Tests showed that sintering occurred if the powder was heated to 850 °C, so the samples were heated to about 650 °C and then cooled rapidly by plunging the quartz tube into water. x-ray investigation using a 9-cm Unicam powder camera showed no extra lines for the 10-at.%-Zn sample. It is well known that the penetration depth for x-rays is very small and it is possible that cooling in this surface region was sufficiently rapid to retain the α phase. Alternatively, the large ratio of surface area to volume might have resulted in enough "sinks" being present to prevent an excess of lattice vacancies occurring on quenching. Further x-ray photographs were taken of more annealed powder samples after holding for 4 weeks at room temperature and at 150 °C, respectively. Again, no extra lines were seen for the 10-at.%-Zn sample.

TABLE II. Analysis of results. Error limits are 95% confidence limits from the statistical analysis, 1 cal = 4.186 J.

Sample (at.% Zn)	Condition	Run	H (μcal °K/ g atom)	γ (μcal/ °K² g atom)	Θ (°K)	B (μcal/ °K⁶ g atom)	Symbol Fig. 1	Symbol Fig. 2
2.5	Slow (furnace) cool	1	0.59±0.07	166.0±0.8	162.5±0.5	−0.30±0.14	■	···
		2	0.59±0.05	165.9±0.7	162.5±0.4	−0.33±0.11	●	···
		Both	0.59±0.04	166.0±0.5	162.5±0.3	−0.31±0.09	···	○
5.0	Fast (air) cool	1	1.02±0.07	168.6±0.8	163.9±0.4	−0.16±0.14	○	···
		2	1.00±0.06	168.5±0.7	163.8±0.4	−0.19±0.12	□	···
		Both	1.01±0.05	168.5±0.5	163.8±0.3	−0.17±0.09	···	○
7.5	Slow (furnace) cool	1	1.45±0.07	168.6±0.9	166.3±0.5	+0.09±0.13	●	···
	Quench from 860 °C	2	1.52±0.08	168.5±0.9	166.3±0.4	+0.03±0.12	■	···
		Both	1.47±0.06	168.6±0.6	166.4±0.3	+0.07±0.10	···	○
10.0	Quench from 825 °C	1	1.77±0.10	153.6±1.1	177.3±0.8	+1.02±0.17[a]	···	···
		2	1.84±0.09	153.2±1.0	176.7±0.7	+0.83±0.15[a]	···	···
		Both	1.80±0.07	153.4±0.7	177.0±0.5	+0.93±0.11[a]	···	△
		3	1.99±0.07	151.8±0.8	176.9±0.5	+0.78±0.13	○	···
	Fast (air) cool	4	1.89±0.07	160.2±0.8	173.3±0.6	+0.53±0.14	●	···
		5	1.99±0.08	157.8±0.9	174.0±0.6	+0.60±0.14	□	·▪
		6	2.02±0.07	156.3±0.8	174.8±0.5	+0.72±0.12	◆	···
	Slow (furnace) cool	7	1.97±0.08	165.8±0.8	170.4±0.5	+0.33±0.12	▼	○
		8	1.96±0.08	164.3±0.9	170.6±0.5	+0.23±0.14	△	···

[a]These results are from Ref. 3 and are not shown in Fig. 1.

It is possible that longer aging would alter the x-ray results or, alternatively, that the changes affecting the specific heat are too short range to show up on the x-ray powder photograph. Also, the composition is so far from stoichiometric that perhaps even under ideal conditions little would be seen on an x-ray powder photograph. It might be argued that the 10-at.%-Zn specific-heat sample has a zinc-rich inclusion which is affecting the specific heat. This seems very unlikely because of the magnitude (~10%) of the effect seen in the specific heat and the fact that analysis of pieces taken from the ends of the sample gave compositions very close to nominal.

Considering the results for the 10-at.%-Zn alloy in conjunction with the others it seems possible that the very slow cool has almost completely retained the α phase (see Fig. 2). If this were so, then the electronic specific-heat results suggest a maximum at about 6 at.%, perhaps supporting Clune and Green's suggestion[2] that one effect (electron-phonon enhancement factor) is superimposed on another (rigid-band model). It will also be seen that the nuclear specific heat hardly depends on the heat treatment of the 10-at.% sample, suggesting that such ordering as does occur has little effect on electric field gradients at nuclear sites.

CONCLUSIONS

The electronic specific-heat coefficient initially increases as zinc is added to gold, the increase being of the magnitude predicted by Clune and Green's argument[2] that variation of the electron-phonon enhancement factor superimposed on the rigid-band model accounts for the electronic specific heat. The results cast doubt on the presently accepted phase diagram for Au-Zn and again emphasize that quenching from high temperatures may be the worst way to attempt to retain a high-temperature phase.

ACKNOWLEDGMENTS

I am indebted to J.W. Fisher for making the alloys, A. Desaulniers and P. Tymchuk (NRCC Analytical Chemistry Section) for the analysis results, R. Boulet for the x-ray work, Mrs. J. MacMillan for computing, and R. Snowdon for help in many ways with the experiments.

[1]T. A. Will and B. A. Green, Phys. Rev. 150, 519 (1966).

[2]L. C. Clune and B. A. Green, Phys. Rev. B 1, 1459 (1970). The explanation is by analogy with results for lead alloys for which the electron-phonon enhancement factor can be determined directly from tunnelling measurements. J. P. Carbotte, P. T. Truant, and R. C. Dynes [Can. J. Phys. 48, 1504 (1970)] have independently shown that the γ variations of aluminum based alloys can be explained in the same way. E. A. Stern [Phys. Rev. B 1, 1518 (1970)] has advanced a rival theory for dilute alloys in which the γ changes are accounted for by shielding of the added impurities.

[3]D. L. Martin, Can. J. Phys. 47, 1077 (1969).

[4]See, for example, N. Waterhouse, Can. J. Phys. 47, 1485 (1969).

[5]D. L. Martin, Phys. Rev. 176, 790 (1968).
[6]D. L. Martin, Phys. Rev. 141, 576 (1966); 170, 650 (1968).
[7]M. Hansen and K. Anderko, *Constitution of Binary Alloys*, (McGraw-Hill, New York, 1958).
[8]R. P. Elliot, *Constitution of Binary Alloys* (McGraw-Hill, New York, 1965), Suppl. 1.
[9]H. Iwasaki, J. Phys. Soc. Japan 17, 1620 (1962).

PHYSICAL REVIEW B VOLUME 4, NUMBER 12 15 DECEMBER 1971

Photoemission from Core States of Cs and Rb†

R. G. Oswald and T. A. Callcott
Department of Physics, The University of Tennessee, Knoxville, Tennessee 37916
(Received 6 July 1971)

Photoemission yields and electron energy distributions of Rb and Cs for photon energies of 12–22 eV are reported. Over most of this energy range, photoexcitation from $np^5(^2P_{3/2})$ $(n+1)s$ and $np^5(^2P_{1/2})$ $(n+1)s$ core levels is observed to be at least two orders of magnitude larger than excitation from the conduction band [$n=4$ (Rb), $n=5$ (Cs)]. Two peaks in the energy distributions which move to higher energy with increasing photon energy result from electrons being directly excited from the shallow core levels. A third peak, which remains stationary in energy position for all photon energies, results from Auger processes which refill the core levels. From the positions and shapes of the peaks, we have obtained values of the spin-orbit splitting of the core levels, the position of the core levels relative to the Fermi (or vacuum) level, and an estimate of the widths of the conduction band. Measurements of spectral yield show a threshold at the core-level–to–Fermi-level spacing that is consistent with this interpretation of structure in the energy distributions. Additional structure in the distributions results when an electron initially excited into one of the above peaks loses energy in exciting a surface plasmon as it escapes through the surface.

I. INTRODUCTION AND CONCLUSIONS

At photon energies below 25 eV, the photoemission process in metals usually involves photoexcitation from the filled portion of the conduction band followed by transport to and escape through the surface. The photoemission studies of Cs and Rb reported by Smith and co-workers, which extended to photon energies of 11.2 eV, followed this pattern.[1,2] At these energies, photoexcitation from rather narrow conduction bands (~1.5 eV for Cs, ~2.0 eV for Rb) injects electrons into higher-band states with this spread of energies. Some of these electrons escape without energy loss to form the highest-energy peak in the external distribution with approximately the width of the filled conduction band. Others escape after electron-electron collisions or after the generation of plasmons degrades their energy. Of particular interest is the fact that some electrons escape after exciting a single surface plasmon, and produce a peak (or shoulder) in the energy distributions displaced below the unscattered peak by the energy of the surface plasmon.

Another feature of interest at energies below 12 eV is that photoemission yields are very low and decrease steadily at photon energies well above the plasma frequency of the alkalies (3 eV in Cs and 3.4 eV in Rb). The low yield results from the fact that at energies above the plasma frequency, the alkalies become nearly transparent so that relatively few electrons are excited sufficiently close to the surface to escape into vacuum. It is well established, both experimentally and theoretically, that the alkalies are nearly free-electron metals with weak and decreasing optical absorption above their plasma frequencies.[3-5] Other absorption mechanisms involving joint excitation of plasmons and electrons have been proposed on the basis of optical measurements, but their existence would not alter the above conclusion that relatively few electrons are excited within the escape depth for photoemission.[5]

The photoemission measurements reported here for photon energies from 12 to 22 eV show many new features not observed at lower energies. Above a threshold of 12.2 eV in Cs and 14.1 eV in Rb, there is a sharply rising increase in yield throughout the entire energy range. Using a detailed analysis of the energy distributions of the electrons contributing to this increased yield, we draw the following conclusions about the processes contributing to photoemission in this energy range:

(a) Two peaks which are visible in our photoemission energy distributions (PED's) result from direct excitation of electrons from two shallow core levels located 12.3 and 14.2 eV below the Fermi level in Cs and 15.3 and 16.4 eV below the Fermi level in Rb. These levels are identified with the $np^5(^2P_{3/2})$ $(n+1)s$ and $np^5(^2P_{1/2})$ $(n+1)s$ excited states observed in the spectra of singly ionized Cs and Rb.[6] The spin-orbit splitting between levels of 1.9 eV for Cs